# Early age monitoring and hardened properties of SCC with limestone filler and active mineral additions

Gonzalo Barluenga [1], Irene Palomar[2] and Javier Puentes [3]

[1] *Professor of Materials and Building Technology, Dep. Architecture, University of Alcala, C/ Santa Úrsula 8, Alcalá de Henares, 28801-Madrid, Spain*
*gonzalo.barluenga@uah.es*
[2] *Architect, PhD Candidate, Dep. Architecture, University of Alcala, C/ Santa Úrsula 8, Alcalá de Henares, 28801-Madrid, Spain,*
*maippe@hotmail.com*
[3] *Architect, PhD Candidate, Dep. Architecture, University of Alcala, C/ Santa Úrsula 8, Alcalá de Henares, 28801-Madrid, Spain,*
*javier.puentes@uah.es*

ABSTRACT:
An experimental program on SCC with limestone filler and three active mineral additions (AMA), microsilica (MS), nanosilica (NS) and Metakaolin (MC), was carried out to evaluate their influence during early ages and in the hardened state. The aim was to characterize SCC further than the usual workability and mechanical parameters, in the understanding that the main microstructural changes in the material occur during the first hours and that early age cracking, porosity, pore size and permeability can compromise SCC durability.

In-situ temperature, ultrasonic pulse velocity, mass loss and free drying shrinkage of samples subjected to a wind flow were simultaneously monitored for 24 hours. Profiles of the reaction process, the microstructural evolution and the physical effects of water evaporation were obtained. The early age measured parameters were related to a reaction index ($I_{r,24}$), defined as the fraction of heat produced (accumulated plus released) with regard to the total heat at 24 hours. The simultaneous monitoring of those parameters allowed a better understanding of the mechanisms involved during early ages. These parameters were compared to the early age cracking due to drying shrinkage.

In the hardened state, a mechanical characterization was conducted and porosity and vapor permeability were measured on paste samples (without aggregates) under two environmental conditions during setting process: subjected to 3 m/s air flow and covered with a plastic film. The use of AMA increased mechanical strength. Although, the early age cracking risks also increased, especially in the case of AMA with smaller particle size (NS and MC). The external conditions applying on the samples during early ages also modify porosity, pore size and permeability of the hardened SCC.

Keywords: Cracking risk, Drying shrinkage, Early age monitoring, Mineral Additions, Mechanical characterization, Porosity, Permeability, Reaction index, UPV.

## INTRODUCTION

SCC compositions are typically characterized by containing a large amount of fine particles, further than the cement used in conventional concretes. Mineral additions (MA), as fillers or active additions (AMA), are of common use as components of SCC in order to increase the amount of paste without using large amounts of cement, specially when moderate strength is required. The use of MA produces changes on the composite performance both the fresh state behavior, as MA modify the workability and rheology, the setting process and the hardened microstructure. These differences not only modify the material performance but can also compromise durability [1-2]. Among the variables that can affect the cement hydration, the nature and particle size of MA can be highlighted [3-8].

Most changes occur in the microstructure during the hydration process and this takes place primarily during the first 12-24 hours. This period of time is usually called early age, which includes the evolution from a liquid dispersion/solution with a plastic behavior (fresh state) into a pseudo-rigid solid (hardened state). Early age is nowadays considered as a key point of the cement based materials evolution, because it enables the material performance in the hardened state and the long term [9].

A proper characterization of cement based materials at early ages requires experimental techniques different to the ones commonly used for fresh or hardened states. Monitoring several parameters, further than just determining setting times, has been proposed to assess the material evolution during early ages [10-13].

The hydration process is usually studied monitoring calorimetric parameters, as temperature or heat released or accumulated by a sample [3-4,10,13-14]. Although, the calorimetric techniques which involve changes on the temperature of the samples can distort the experimental results of the hydration process. The microstructure evolution can be followed monitoring the changes of ultrasonic pulse velocity (UPV) through samples under defined environmental conditions [10-13,15-16]. The combination of both parameters allows to identify the main changes of the material during early ages [11-13,15-16].

MA have been reported to modify the material evolution at early ages through two main mechanisms: facilitating the nucleation of hydrated cement products, as fillers and non-active MA [3-5], and reacting with portlandite due to pozzolanic activity, as AMA [6-8,13], producing calcium silicate hydrates (CSH) [6-7] and aluminates [8,13].

The environmental conditions greatly affect the development of hydration during early ages and determine the microstructure evolution and the hardened performance [8,13]. Temperature can modify the speed of the reaction and, jointly with relative humidity and wind velocity, can force water evaporation and drying shrinkage. The typical consequence of the environmental influence on early age concrete performance, further than reaction speed, is cracking due to drying shrinkage [1-2,17-19].

Cracking happens when a concrete member simultaneously has its displacement restrained, suffers a dimensional change, has a certain stiffness and the (tensional) stress overcomes the mechanical capacity of the member. In the case of early age cracking due to drying shrinkage, the dimensional change is related to water evaporation and the formation of menisci inside the (pseudo-solid) pore structure and the stiffness and mechanical capacity only develops when a certain degree of interconnected (pseudo-rigid) microstructure is achieved [13,15]. Early age stiffness has been described to be related to a mechanism of grain interconnection while strength development depends on pore filling by hydration products. Therefore, cracking due to early age drying shrinkage is linked to reaction development, microstructure evolution and environmental effects.

As far as shrinkage depends on paste hydration and water evaporation, SCC are specially susceptible to crack at early age, because SCC usually has larger amount of paste and water than any conventional concrete. However, SCC has been described to show similar cracking risks than conventional concretes at early ages [1,2]. In any case, early age cracking of SCC is still an issue to be considered, as far as it can compromise durability.

Another consequence of the influence of MA in SCC performance to be considered is the pore microstructure of the hardened composite, which is mainly formed during early age and determine their performance, both physically and mechanically, and can also compromise their durability, because MA can modify pore size, porosity and permeability [20].

## EXPERIMENTAL WORK

An experimental program on fluid pastes and SCC with several AMA was carried out. Limestone filler (CA), microsilica (MS), nanosilica (NS) and metakaolin (MC) were considered. The aim of the study was to assess the influence of SCC composition at early ages and in the hardened state and to identify the relationships between both stages. At early ages, the hydration process, the microstructure evolution, the heat and water interchanges with the environment and the free drying shrinkage were simultaneously monitored. The cracking risks linked to early age shrinkage were also considered. In the hardened state, the physical and mechanical performance was characterized and the porosity and vapor permeability were measured.

### Materials and mix proportions

The concrete compositions used in this study are summarized in Table 1. A reference concrete, without a High range water reducing admixture (HRWRA) and a dry consistency, was considered (named HREF). This reference composition was modified including a HRWRA and achieving a self compacting ability (HREFG). Afterwards, 50 % of the cement was substituted by limestone filler, obtaining a conventional SCC with filler (HCA). Three active mineral additions were studied, manufacturing compositions where 5 to 10 % of the limestone filler was substituted by microsilica (HCAMS), nanosilica (HCANS) and Metakaolin (HCAMC). The water to fines ration (w/f) remained at 0.36 for all the compositions and the amount of paste was constant in all cases. As far as the SCC performance highly depends on paste properties, samples of the six different pastes were also tested.

Table 1 also records the slump of the REF composition (dry consistency) and the average slump spread diameter and the blocking coefficient of the reference SCC composition and the conventional limestone filler SCC. No segregation or bleeding was observed on the samples in the fresh state.

Table 1 ─Compositions of the SCC mixtures under study (components in Kg/m3).

| Compositions | HREF | HREF G | HCA | HCAMS | HCANS | HCAMC |
|---|---|---|---|---|---|---|
| Cement CEM I 42,5 R | 700 | 700 | 350 | 350 | 350 | 350 |
| Siliceous Gravel (4-20 mm) | 790 | 790 | 790 | 790 | 790 | 790 |
| Siliceous Sand (0-4 mm) Humidity 6.25 % | 691 | 691 | 691 | 691 | 691 | 691 |
| Limestone Filler (Betocarb P1-DA) | - | - | 350 | 315 | 332.50 | 332.50 |
| Micro-silica (MEYCO MS 610) | - | - | - | 35 | - | - |
| Nano-silica (MEYCO MS 685) | - | - | - | - | 79.45 | - |
| Metakaolin (Burgess Optipozz) | - | - | - | - | - | 17.50 |
| Water (*) | 209.25 | 198.75 | 204 | 204 | 142 | 204 |
| HRWRA (Glenium ACE425) | - | 10.50 | 5.25 | 5.25 | 5.25 | 5.25 |
| W/c (**) | 0.36 | 0.36 | 0.71 | 0.71 | 0.71 | 0.71 |
| W/fines (cement + additions) (**) | 0.36 | 0.36 | 0.36 | 0.36 | 0.36 | 0.36 |
| Slump Cone (mm) | 24 | - | - | - | - | - |
| J-ring djf(***) mm | - | 875 | 815 | - | - | - |
| CbE(***) % | - | 37 % | 29 % | - | - | - |

(*) Liquid water added.
(**)The amount of water included in the components (sand, HRWRA and nano-silica) was also considered.
(***)UNE 83362:2007- Self-compacting concrete. Characterization of the flowability through rebars. Slump-flow test with J-ring.

### Early age measurements

Internal temperature and p-wave ultrasonic pulse velocity (UPV) was monitored on 150 x 100 x 70 mm concrete samples at laboratory conditions (20±2 ºC, 50±10 % relative humidity) during 24 hours. The samples were cast in a plastic mold and the upper surface of the samples was in direct contact with the environment. Although the direct temperature measurement is less accurate than other techniques (isothermal and semi-adiabatic calorimetry), this procedure does not modify the thermal profile of the samples, which could alter the reaction speed [3,13,16].

A free shrinkage apparatus with internal dimensions of 500 x 100 x 50 mm, subjected to an air flow of 3 m/s during 6 hours, were used to monitor free drying shrinkage simultaneously. The evaporation rate was calculated, measuring the mass loss of the samples, placing the shrinkage apparatus on a continuous recording scale.

Cracking risks due to drying shrinkage at early ages was evaluated on two types of slabs: 400 x 400 x 40 mm y de 600 x 900 x 50 mm (modified Kraai slab test [1]). U-shaped steel pieces were attached inside the molds in order to avoid horizontal displacements. The slabs were subjected to an air flow of 3 m/s to force cracking due to drying shrinkage. The experimental setup of shrinkage, evaporation and cracking test have been previously described [1,13].

Characterization in the hardened state

In the hardened state, density, UPV and Ultrasonic modulus, compressive strength, porosity and vapor permeability were characterized. Apparent density of hardened SCC samples and UPV measurements were measured on cubic specimens of 100 mm. Porosity and average pore diameter [20] were measured using an mercury intrusion porosimeter on paste samples extracted from the free shrinkage specimens under air flow and covered with a plastic film. Vapor permeability and permeability coefficient was calculated from samples tested according to UNE-EN 15.803 Spanish-European standard, also extracted from the free shrinkage specimens under air flow and covered with a plastic film.

## EXPERIMENTAL RESULTS

Early age results

Figure 1 summarizes temperature, UPV and free drying shrinkage of the six concrete compositions considered in this study.

The temperature changes of the samples are related to the hydration reactions (exothermic) and the pozzolanic reactions when AMA were considered. In all the compositions under study, the temperature of the samples was higher than the environment during the test (24 hours). Four stages can be identified in the temperature curve for all the compositions. After a first stage of temperature decrease, commonly known as dormant period, the temperature increase due to the acceleration of the hydration process (second stage). A third stage corresponded to a constant increase until a maximum was reached and in the last stage a slow cool down occurred. It can be observed that the use of HRWRA (HREFG) delayed the acceleration period with regard to the reference composition without admixture (HREF). In contrast, the substitution of 50 % of cement by filler reduced the retardant effect of the HRWRA. On the other hand, the AMA increased the maximum temperature with regard to the SCC with filler.

UPV curves also showed a pattern, with a first stage of fresh state with a constant value (which corresponded to the velocity through the aggregate grains), a second stage of rapid increase, which corresponded to the transition between fresh and hardened (semi-rigid state), and a third stage of slow down increase, when the sample was already rigid [13,16].

Free drying shrinkage curves of samples under an air flow of 3 m/s during the first 6 hours can also be described with a first stage where the apparatus did not record any measurement (plastic shrinkage), then an accelerated increase occurred, in a third stage an inflection point (“knee point”) is reached and a decelerated increase happened, corresponding to material hardening, until stabilization. Evaporation data of the shrinkage samples are presented in Table 2. As far as the paste samples covered with a plastic film did not record any shrinkage, it was concluded that all the shrinkage recorded corresponded to drying.

A relation among temperature, UPV and shrinkage can be observed in all the cases, as far as the rapid increase of UPV corresponded to the acceleration period of the temperature. The free drying shrinkage began during the dormant period and got stabilized during the acceleration period in the samples with limestone filler. The reference compositions (HREF and HREFG) showed a stabilized shrinkage before acceleration period.

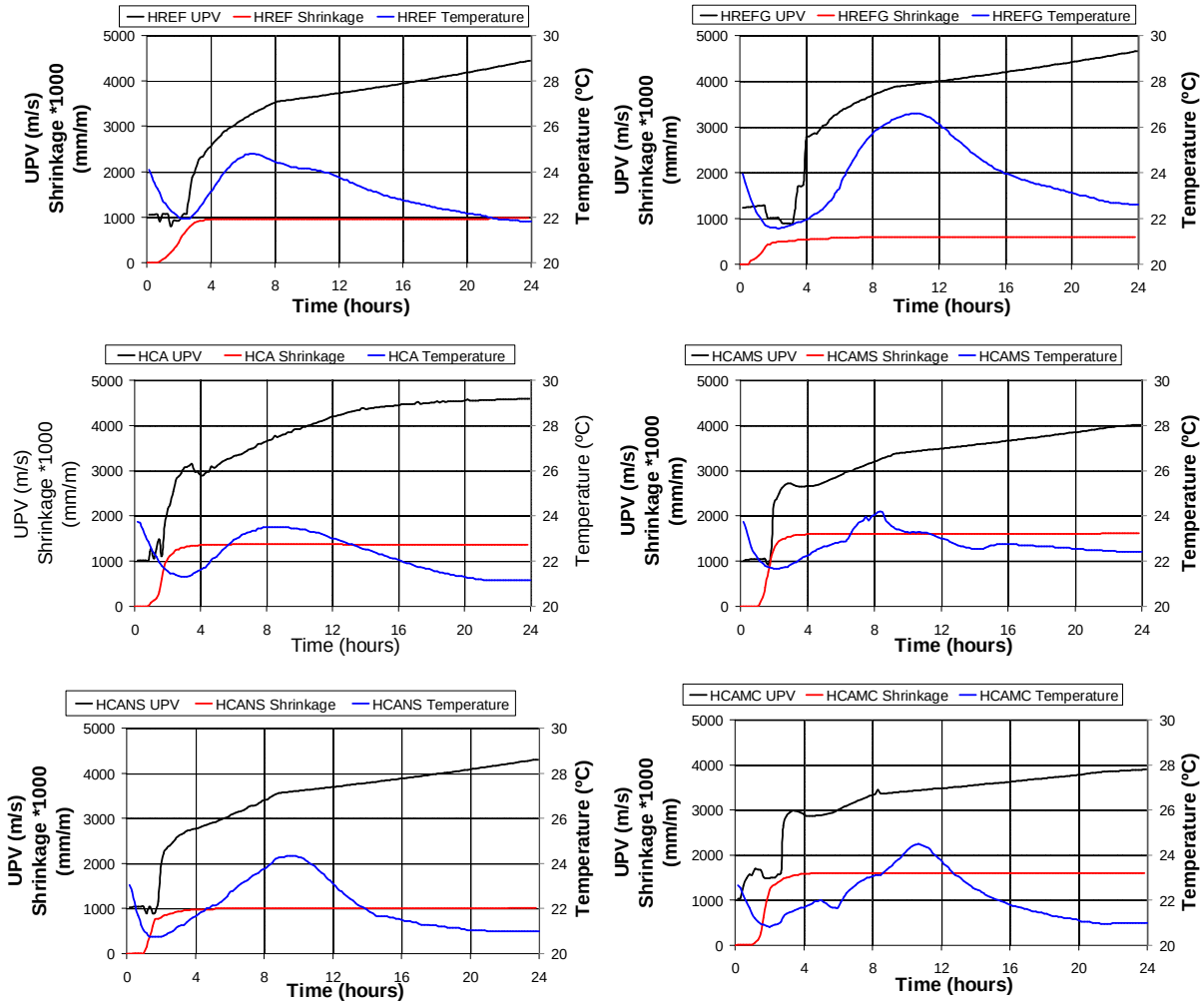


Figure 1 — Temperature, UPV and free drying shrinkage (6 hours under 3 m/s air flow) of SCC samples.

Table 2 –Key points of evaporation and drying shrinkage tests at early age and slab cracking test results.

| | | HREF | HREF G | HCA | HCAMS | HCANS | HCAMC |
|---|---|---|---|---|---|---|---|
| Evaporation | | | | | | | |
| Initial time (minutes) | | 60 | 20 | 70 | 20 | 20 | 20 |
| Evaporation (kg/m$^2$) at 6 hours | | 1.50 | 2.12 | 1.64 | 1.22 | 2.48 | 2.36 |
| Drying Shrinkage (air flow 3 m/s) | | | | | | | |
| Shrinkage at "Knee" point (mm/m) | | 0.56 | 0.28 | 0.92 | 0.76 | 0.60 | 0.62 |
| Maximum shrinkage (mm/m) | | 0.98 | 0.60 | 1.38 | 1.62 | 1.02 | 1.60 |
| Laboratory conditions (temp (ºC)/ RH (%)) | | 21 / 50 | 21 / 52 | 20.5 / 50 | 21 / 50 | 20 / 52 | 20 / 55 |
| Slab cracking tests | | | | | | | |
| Slab 400x400 mm | Cracked area (mm$^2$/m$^2$) | 5.92 | 150.23 | 43.72 | 402.37 | 356.34 | 1188.30 |
| | Max. crack length (mm) | 18 | 50 | 51 | 35 | 34 | 178 |
| Kraai modified (900 x 600 mm) | Cracked area (mm$^2$/m$^2$) | 2.41 | - | 344.63 | 1270.74 | 1923.15 | 536.02 |
| | Max. crack length (mm) | 26 | - | 275 | 85 | 80 | 95 |

The results of evaporation, drying shrinkage and forced cracking on the two types of slab tests are summarized in Table 2. It can be observed that there is no direct relation among them, as far as larger evaporation did not mean

larger shrinkage or cracking risk. The only exception is the composition with metakaolin (HACMC) which presents the largest evaporation, shrinkage and cracking measurements. Regarding cracking risk, the results were quite different depending on the type of slab considered, although a general trend can be observed. The reference compositions presented lower risks of cracking while the compositions with AMA showed larger cracked area.

Hardened State results

The hardened state performance was characterized on cubic samples of 100 mm. Apparent density, compressive strength, UPV and ultrasonic modulus, calculated according to the literature [13], are recorded in Table 3. The use of AMA slightly reduced apparent density and ultrasonic modulus, while increased compressive strength, mainly in the compositions with nanosilica (HCANS) and Metakaolin (HCAMC).

Table 3 –Physical and Mechanical properties of hardened SCC samples at 28 days.

| | HREF | HREF G | HCA | HCAMS | HCANS | HCAMC |
|---|---|---|---|---|---|---|
| Apparent density (g/cm3) | 2.35 | 2.38 | 2.31 | 2.33 | 2.31 | 2.25 |
| Compressive Strength (MPa) | 44.30 | 55.88 | 31.50 | 33.48 | 39.05 | 39.25 |
| US modulus (GPa) | 46.32 | 52.61 | 50.18 | 52.74 | 44.09 | 46.91 |
| UPV (m/s) | 4439.75 | 4701.50 | 4660.75 | 4757.50 | 4369 | 4566 |

Figure 2 plots the compressive strength during the first 28 days. It can be observed that the reference mixtures (HREF, HREFG) and the composition with filler (HCA) showed the same curve pattern, taking into account that the amount of cement is 50% less in the last case. The samples with AMA presented a different pattern, as far as compressive strength was lower at 1 day and the increase during the interval from 1 to 28 days was faster than the samples only with filler. It has been described in the literature that the evidences of the pozzolanic activity of AMA are easily recognizable between 7 and 28 days [8].

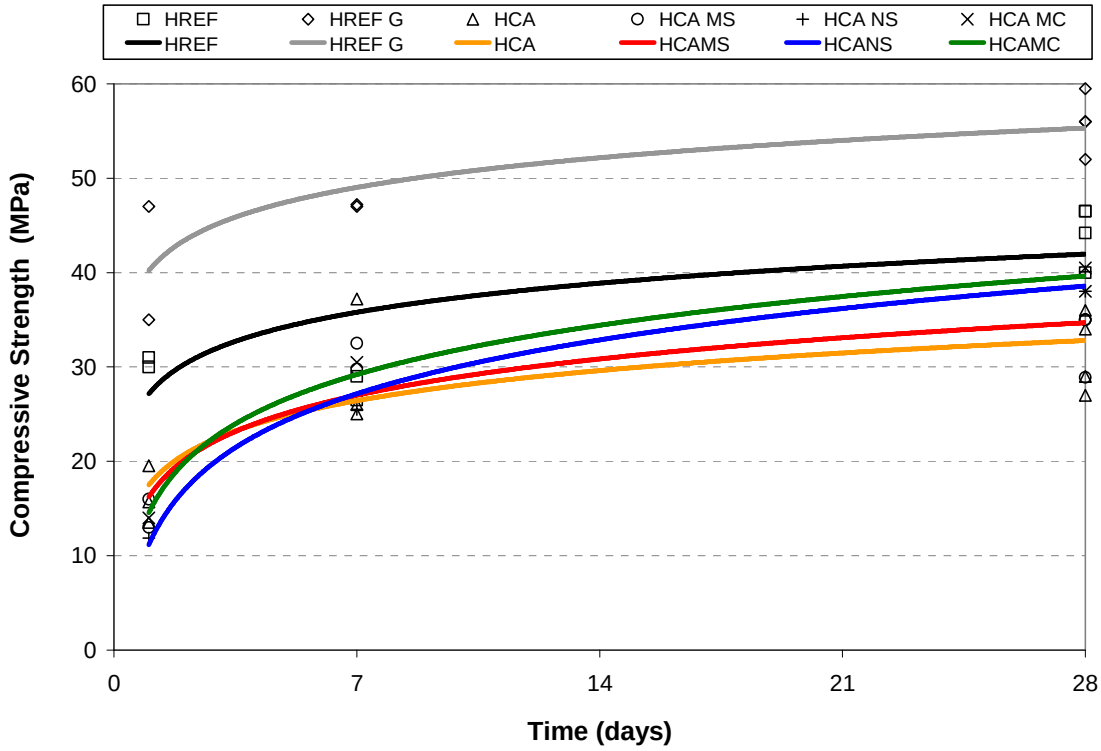


Figure 2 — Compressive strength of concrete samples at 1, 7 and 28 days (water cured).

Table 4 summarizes the values of porosity and average pore diameter, permeability and permeability coefficient of samples extracted from free shrinkage paste specimens submitted to an air flow and covered with a plastic film, respectively. The porosity of the compositions under study is low and the samples covered with a plastic film during setting present larger porosity and lower average pore diameter. The samples with AMA showed lower porosity and average pore diameter. The permeability coefficient and the permeability also followed the same pattern.

Table 4 ─Porosity and average pore diameter (Mercury porosimetry), vapor permeability coefficient and permeability of pastes under air flow and covered with a plastic film.

| | Average D (μ) | Porosity (%) | Permeability Coeff. ($g/m^2$ 24h.mmHg) | Permeability ($g/m^2$.h cm) |
|---|---|---|---|---|
| Air flow samples | | | | |
| REF V | 0.6714 | 7.21 | 0.44 | 3.06 |
| REFG V | 0.3635 | 7.60 | 0.51 | 3.18 |
| CA V | 0.5839 | 8.92 | 0.61 | 4.47 |
| CAMS V | 0.5894 | 8.83 | 0.58 | 5.94 |
| CANS V | 0.4166 | 5.02 | 0.44 | 3.06 |
| CAMC V | 0.3677 | 6.48 | 0.45 | 2.09 |
| Covered samples | | | | |
| REF T | 0.1545 | 10.64 | 0.63 | 3.36 |
| REFG T | 0.1561 | 9.15 | 0.58 | 2.41 |
| CA T | 0.3797 | 9.47 | 0.77 | 4.49 |
| CAMS T | 0.3209 | 5.99 | 0.51 | 4.59 |
| CANS T | 0.2912 | 7.90 | 0.55 | 4.35 |
| CAMC T | 0.3568 | 8.39 | 0.53 | 3.66 |

## ANALYSIS AND DISCUSSION

Relations among Early age parameters

The early age results obtained for the compositions under study are difficult to compare among them, because the main events of the process do not coincide in time. In order to facilitate the comparison, a new parameter can be defined regarding the hydration evolution.

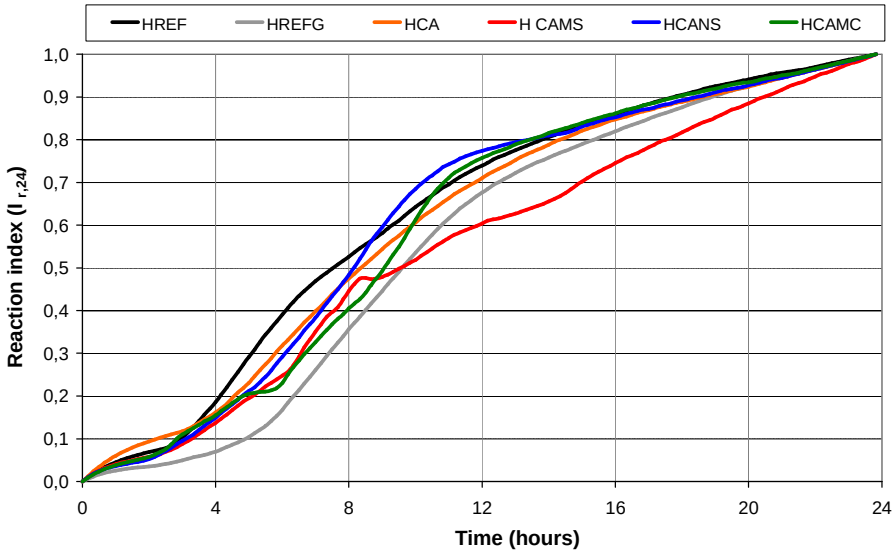


Figure 3 — Reaction Index ($I_{r,24}$) of SCC samples.

Taking the temperature curves and considering that the temperature of the samples was higher than the environment during the test (24 hours), the amount of heat produced during the hydration can be estimated as the sum of heat accumulated by the sample and the heat released to the environment [16]. Thereby, a reaction index ($I_{r,24}$) can be defined as the fraction of heat produced by the sample until a certain moment with regard to the total heat produced at 24 hours [16]. The $I_{r,24}$ of the compositions under study during the first 24 hours are plotted in Figure 3. The reference mixture without HRWRA presents a faster development of $I_{r,24}$, followed by the compositions with filler and AMA. The reference mixture with HRWRA presents a delay of the reaction. All the samples show an S-shape curve, with a first part of low increase, then a rapid increase and around 12 hours (maximum value of temperature) another phase of low increase.

Figure 4 plots UPV related to $I_{r,24}$, and the three main stages of the microstructure evolution can be identify: plastic state, semi-rigid and rigid [15]. It can be observed that the transition from plastic to rigid is very fast, with values of $I_{r,24}$ between 0.05 and 0.1. The compositions with MS and NS presented the earlier transition while the reference composition without HRWRA (HREFG) and the SCC only with filler (HCA) were the last.

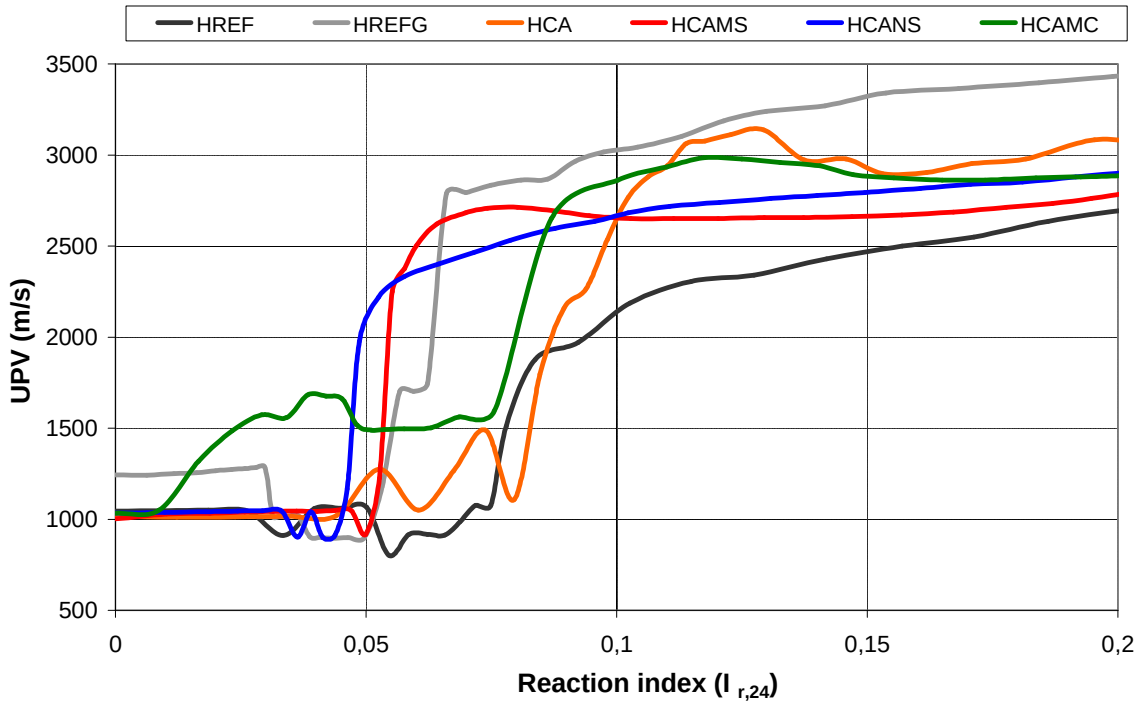


Figure 4 — Ultrasonic Pulse Velocity (UPV) vs Reaction Index ($I_{r,24}$) of SCC samples at very early ages.

The relation between free drying shrinkage and $I_{r,24}$ is plotted in Figure 5. In this case, the development of the measured shrinkage also occurred at a very low $I_{r,24}$, with values between 0.05 and 0.1. Although, it must be taken into account that $I_{r,24}$ and UPV depend on the hydration process and the microstructure evolution, while drying shrinkage also depend on evaporation, as far as the samples of paste covered with a plastic film did not lose water and, therefore, did not record any drying shrinkage [13].

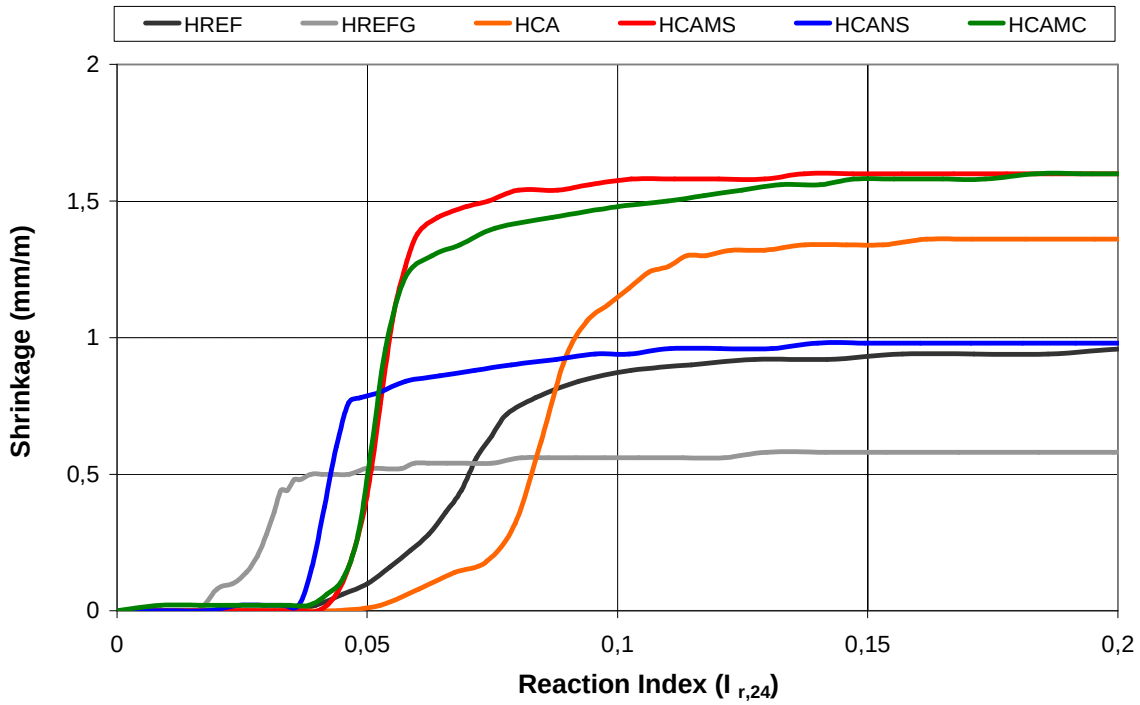


Figure 5 — Drying shrinkage vs Reaction Index ($I_{r,24}$) of SCC samples at very early ages.

Summarizing and according to the experimental results, it can be said that the use of filler and AMA modified the early age performance. The hydration of the cement (HREF) was altered by the inclusion of the HRWRA (HREFG) and the limestone filler (HCA), as far as the admixture delayed the thermal process while the use of filler attenuates the delay [3,4] (Figure 3). Accordingly, when $I_{r,24}$ is related to microstructure development (Figure 4), the samples with filler showed a higher $I_{r,24}$ when the transition from plastic to rigid states occurred. The SCC samples with AMA partially modified the behavior observed for the samples only with filler, as far as the pozzolanic reactions occurred when the temperature was already increasing [13]. MS and NS, both silica-based additions, produced the maximum temperature before the sample with MC, which is an aluminates-based addition and reacted later [8]. As a consequence, the transition from plastic to rigid states happened before, especially in the case of the AMA with smaller size particles (NS and MC).

The environmental conditions surrounding the samples also affect the early age performance [2,8,13]. In this study, only the air flow was considered as an environmental variable, while the temperature and relative humidity remained practically constant (Table 2). The samples with NS and MC showed the maximum evaporation, overcoming the evaporation of the reference composition with HRWRA, while the compositions with filler and with MS presented lower evaporation (Table 2). It can be noted that these results agree with the evaporation of paste samples [13]. The drying shrinkage measurements were not proportional to evaporation. In fact, evaporation began before shrinkage for all the compositions. It can be explained considering that the mass loss that occurred before a minimum interconnection among the solid particles took place in a plastic state, which can be accommodated plastically ad was not recorded by the shrinkage apparatus.

On the other hand, the coincidence between UPV and drying shrinkage rapid evolution points out that the transition between plastic and rigid state can be detected with both parameters. At this moment, when the material reached a rigid state and the evaporation increase shrinkage, tensional stress could develop, which can overcome tensional strength and produce cracking. It was observed that the inclusion of filler and AMA increased cracking risks due to drying shrinkage. The different results obtained with the two types of slab tests could be explained on the different cracking propagation mechanisms due to the thickness of sample over the metallic pieces embedded inside the slabs.

Hardened state performance

The samples with AMA showed larger compressive strength than the composition only with limestone filler (HCA), as it can be observed in Table 3. AMA with smaller particle size (NS and MC) presented an increase around 20 %. The increase of compressive strength from 1 to 28 days was also larger for samples with AMA than the reference compositions. This fact can be explained considering the pozzolanic activity of AMA and the expected effect during this age. Although, the increase of strength did not produce a larger stiffness, as far as the ultrasonic modulus was lower for these compositions (HCANS and HCAMC), while the samples with MS presented larger ultrasonic modulus.

The particle size of the AMA also looked to have influence in the porosity and vapor permeability measurements (Table 4). The use of AMA reduced the average pore diameter and the porosity with regard to the SCC composition only with limestone filler. This fact is specially evident for the samples covered with a plastic film, where all the pores are filled with water and the hydration products could crystallize inside them. The results of vapour permeability also pointed out to a reduction when AMA were used. Vapor permeability coefficient was reduced for both exposed to wind and covered samples.

Against expectations, both porosity and vapor permeability increased for samples covered with a plastic film with regard to the samples subjected to forced evaporation. Only the composition with MS showed larger porosity and permeability for wind exposed samples. It can be explained considering that covered samples did not lose water due to evaporation and that all the unreacted water remained inside the sample, occupying space. After hardening, the water would escape to the exterior but the pores would remain in the hardened microstructure. Although the average pore diameter is smaller for covered samples due to the crystallization of hydration products inside the pores, but vapor permeability increased. Therefore, it can be said that vapor permeability depended on porosity, which is larger for covered samples, rather than average pore diameter, which affects water permeability [20].

## CONCLUSIONS

An experimental program on SCC with limestone filler and active mineral additions (AMA) was carried out, monitoring some early age parameters and characterizing the hardened strength, UPV, porosity and vapor permeability. Microsilica (MS), Nanosilica (NS) and Metakaolin (MK) were considered. The main conclusions were:

(1) The simultaneous monitoring of several parameters (temperature, UPV, mass loss and free drying shrinkage) allowed a better understanding of the mechanisms involved during SCC early ages.

(2) The inclusion of AMA produced changes on SCC performance at early ages and in the hardened state: AMA increased mechanical strength and modified porosity and permeability, although the early age cracking risks due to drying shrinkage also increased, specially in the case of AMA with smaller particle size (NS and MC).

(3) At early ages, limestone filler accelerated the speed of hydration, and the use of AMA did not significantly modify this effect. The index of reaction ($I_{r,24}$), defined as the fraction of heat produced (accumulated plus released) with regard to total heat at 24 hours, was lower for samples with AMA when the microstructure changes began, with regard to the reference mixture with superplasticiser.

(4) Limestone filler and MS reduced water evaporation, while NS and MC increased it. Although, drying shrinkage did not follow evaporation, as MS and MC increased it.

(5) NS and MC produced the larger cracking risk, because the main UPV change occurred after drying shrinkage began to stabilize.

(6) The external conditions applying on the paste samples during early ages modified porosity, average pore diameter and vapor permeability of the hardened SCC.

(7) For the compositions under study it was observed that the larger the evaporation, the lower the porosity and the permeability, although the average pore diameter increased.

(8) The paste samples covered with a plastic film did not show water evaporation and the average pore diameter decrease with regard to the samples exposed to an air flow. However, porosity also increased and so did vapor permeability, as vapor permeability depends on porosity rather than pore size.

## ACKNOWLEDGEMENTS

The authors gratefully acknowledge the contribution on the samples preparation and testing of the students Alvaro Mozas and Hector Arenas, as well as the technical support of R. Tascón, G. Sánchez and I. Pajares. Some of the components were supplied by BASF Construction Chemicals España S.L., Omya Clariana SL and Cementos Portland Valderrivas. Financial support for this research was provided by the grant CCG-08-UAH/MAT 4038, co-funded by University of Alcalá and the Comunidad de Madrid; PI3-2008-0499, funded by the Spanish Ministry of Science and Innovation; PII-11-0167-3491, funded by the Junta de Comunidades de Castilla La Mancha, and the Research Program Geomateriales (S2009/Mat-1629), funded by the Comunidad de Madrid.

## REFERENCES

1. Barluenga, G.; Hernandez-Olivares, F., "Cracking control of concretes modified with short AR-glass fibers at early age: Experimental results on standard concrete and SCC", Cement and Concrete Research V. 37, No. 12, 2007, pp. 1624-1638.

2. Barluenga, G., "Fiber–matrix interaction at early ages of concrete with short fibers", Cement and Concrete Research, V. 40, 2010, pp. 802–809.

3. Poppe, A-M; De Schutter, G., "Cement hydration in the presence of high filler contents", *Cement and Concrete Research,* V. 35, 2005, pp. 2290 – 2299.

4. Ye, G.; Liu, X.; Poppe, A. M.; De Schutter, G.; van Breugel, K., "Numerical simulation of the hydration process and the development of microstructure of self-compacting cement paste containing limestone as filler", Materials and Structures, V. 40, 2007, pp.865–875.

5. Kadri, E. H.; Aggoun, S.; De Schutter, G.; Ezziane, K., "Combined effect of chemical nature and fineness of mineral powders on Portland cement hydration", Materials and Structures, V. 43, 2010, pp. 665–673.

6. Senff, L.; Hotza, D; Repette, W L.; Ferreira, V M.; Labrincha, J A., "Mortars with nano-SiO2 and micro-SiO2 investigated by experimental design", Construction and Building Materials, V. 24, 2010, pp.1432–1437.

7. Gaitero, J.J.; Campillo, I.; Guerrero, A., "Reduction of the calcium leaching rate of cement paste by addition of silica nanoparticles". Cement and Concrete Research, V. 38, 2008, pp.1112–1118.

8. Siddique, R.; Klaus, J., "Influence of metakaolin on the properties of mortar and concrete: A review", Applied Clay Science, V. 43, 2009, pp. 392–400.

9. Bentz, D.P, "A review of early-age properties of cement-based materials", Cement and Concrete Research, V. 38, 2008, pp.196–204.

10. Desmet, B.; Atitung, K. C.; Abril Sanchez, M. A.; Vantomme, J; Feys, D.; Robeyst, N.; Katrien Audenaert, K.; De Schutter; G.; Boel, V.; Heirman; G.; Cizer, Ö.; Vandewalle, L.; Van Gemert, D., "Monitoring the early-age hydration of self-compacting concrete using ultrasonic p-wave transmission and isothermal calorimetry", Materials and Structures, V. 44, 2011, pp. 1537-1558.

11. Barluenga, G.; Palomar, I.; Puentes, J., "Estudio de comportamiento a edades tempranas de Hormigones Autocompactantes", Proc. II National Spanish Congress on Building Research. UPM, EUAT, D.L. 2010.pp. 1-10.

12. Darquennes, A.; Khokhar, M.I.A.; Rozière, E.; Loukili, A.; Grondin, F.; Staquet, S., "Early age deformations of concrete with high content of mineral additions", Construction and Building Materials, V. 25, 2011 , pp. 1836–1847.

13. Barluenga, G.; Palomar, I.; Puentes, J., "Early age and hardened performance of fluid cement pastes combining mineral additions", Materials and Structures, 2012, pp. 1-21 (on line Oct. 2012).

14. Hesse, C.; Goetz-Neunhoeffer, F; Neubauer, J, "A new approach in quantitative in-situ XRD of cement pastes: Correlation of heat flow curves with early hydration reactions". Cement and Concrete Research, V. 41, 2011, pp. 123–128.

15. Boumiz, A.; Vernet, C.; Cohen Tenouj, F., "Mechanical Properties of Cement Pastes and Mortars at Early Ages - Evolution with Time and Degree of Hydration", Advanced Cement Based Materials, V. 3, 1996, pp. 94-106.

16. Robeyst, N.; Gruyaert, E.; Grosse, C.U.; De Belie, N., "Monitoring the setting of concrete containing blast-furnace slag by measuring the ultrasonic p-wave velocity", Cement and Concrete Research, V. 38, 2008, pp. 1169-1176.

17. Uno, P., "Plastic Shrinkage Cracking and Evaporation Formulas". ACI Materials Journal, V. 95, No. 4, 1998, pp. 365-375.

18. Kraai, P. P., "A proposed test to determine the cracking potential due to drying shrinkage of concrete", Concrete Construction, V. 9, No. 30, 1985, pp. 775-778.

19. Holt, E.; Leivo, M., "Cracking risks associated with early age shrinkage", Cement and Concrete Composites, V. 26, No. 5, 2004, pp. 521-530.

20. Bermejo, E. B.; Moragues, A.; Galvez, J. C.; Fernandez Canovas, M., "Permeability and pore size distribution in medium strength self-compacting concrete", Materiales de Construccion, V. 60,No. 299, 2010, pp. 37-51.